

A&A manuscript no.
 (will be inserted by hand later)
Your thesaurus codes are:
02.08.1 02.20.1 09.03.1; 09.07.1; 09.11.1; 09.19.1;

**ASTRONOMY
 AND
 ASTROPHYSICS**

N-body simulations of self-gravitating gas in stationary fragmented state

B. Semelin and F. Combes

Observatoire de Paris, DEMIRM, 61 Av. de l'Observatoire, F-75014, Paris, France

Received XX XX, 1999; accepted XX XX, 2000

Abstract. The interstellar medium is observed in a hierarchical fractal structure over several orders of magnitude in scale. Aiming to understand the origin of this structure, we carry out numerical simulations of molecular cloud fragmentation, taking into account self-gravity, dissipation and energy input. Self-gravity is computed through a tree code, with fully or quasi periodic boundary conditions. Energy dissipation is introduced through cloud-cloud inelastic collisions. Several schemes are tested for the energy input. It appears that energy input from galactic shear allows to achieve a stationary clumped state for the gas, avoiding final collapse. When a stationary turbulent cascade is established, it is possible to derive meaningful statistical studies on the data such as the fractal dimension of the mass distribution.

Key words: Physical processes: Hydrodynamics – Physical processes: Turbulence – ISM: clouds – ISM: general – ISM: kinematics and dynamics – ISM: structure

1. Introduction

From many studies over the last two decades, it has been established that the interstellar medium (ISM) has a clumpy hierarchical structure, approaching a fractal structure independent of scale over 4 to 6 orders of magnitude in sizes (Larson 1981, Scalo 1985, Falgarone et al 1992, Heithausen et al 1998). The structure extends up to giant molecular clouds (GMC) of 100 pc scale, and possibly down to 10 AU scale, as revealed by HI absorption VLBI (Diamond et al 1989, Faison et al 1998) or extreme scattering events in quasar monitoring (Fiedler et al. 1987, Fiedler et al. 1994). It is not yet clear which mechanism is the main responsible for this structure; it could be driven by turbulence, since the Reynolds number is very high, or self-gravity, since clouds appear to be virialized on most of the scales, with the help of magnetic fields, differential rotation, etc...

One problem of the ISM turbulence is that the relative velocities of clumps are supersonic, leading to high dissip-

tion, and short lifetime of the structures. An energy source should then be provided to maintain the turbulence. It could be provided by star formation (stellar winds, bipolar flows, supernovae, etc... Norman & Silk 1980). However, the power-law relations observed between size and line-width, for example, are the same in regions of star-formation or quiescent regions, either in the galactic disk, or even outside of the optical disk, in the large HI extensions, where very little star formation occurs. In these last regions alternative processes of energy input must be available. A first possiblity is the injection by the galactic shear. Additionally, since there is no heating sources in the gas, the dense cold clumps should be bathing at least in the cosmological background radiation, at a temperature of 3K (Pfenniger & Combes 1994). In any case, in a nearly isothermal regime, the ISM should fragment recursively (e.g. Hoyle 1953), and be Jeans unstable at every scale, down to the smallest fragments, where the cooling time becomes of the same order as the collapse time, i.e. when a quasi-adiabatic regime is reached (Rees 1976).

In this work, we try to investigate the effect of self-gravity through N-body simulations. We are not interested in star formation, but essentially in the fractal structure formation, that could be driven essentially by gravity (e.g. de Vega et al. 1996). Our aim is to reach a quasi-stationary state, where there is statistical equilibrium between coalescence and fragmentation of the clouds. This is possible when the cooling (energy dissipated through cloud collisions, and subsequent radiation) is compensated by an energy flux due to external sources : cosmic rays, star formation, differential shear... Previous simulations of ISM fragmentation have been performed to study the formation of condensed cores, some with isolated boundary conditions (where the cloud globally collapses and forms stars, e.g. Boss 1997, Burkert et al. 1997), or in periodic boundary conditions (Klessen 1997, Klessen et al. 1998). The latter authors assume that the cloud at large scale is stable, supported by turbulence, or other processes. They follow the over-densities in a given range of scales, and schematically stop the condensed cores as sink particles when they should form structures below their resolution. We also adopt periodic boundary conditions, since numer-

ical simulations are very limited in their scale dynamics, and we can only consider scales much smaller than the large-scale cut-off of the fractal structure. We are also limited by our spatial resolution: the smallest scale considered is far larger than the physical small-scale cut-off of the structures. Our dynamics is computed within this range of scales.

Our goal is to achieve long enough integration time for the system to reach a stationary state, stationary in a statistical sense. This state should have its energy confined in a narrow domain, thus presenting the density contrasts of a fragmented medium while avoiding gravitational collapse after a few dynamical times. Only when those conditions are fulfilled, can we try to build a meaningful model of the gas. Let us consider for example the turbulence concepts.

Theoretical attempts have been made to describe the interstellar medium as a turbulent system. While dealing with a system both self-gravitating and compressible, the standard approach has been to adapt Kolmogorov picture of incompressible turbulence. The first classical assumption is that the rate of energy transfer between scales is constant within the so-called inertial range. This inertial range is delimited by a dissipative scale range at small scales and a large scale where energy is fed into the system. In the case of the interstellar medium, the energy source can be the galactic shear, or the galactic magnetic field, or, on smaller scales, stellar winds and such. In this classical picture of turbulence, one derives the relation $v_L \sim L^{1/3}$, where v_L is the velocity of structures on scale L . If we consider now that the structures are virialized at all scales, we get the relation $\rho_L \sim L^{-4/3}$, where ρ_L is the density of structures on scale L . This produces a fractal dimension $D = 1.66$. A more consistent version is to take compressibility into account in Kolmogorov cascade; then $\rho_L v_L^3 / L \sim cst$. Adding virialization, we get the relations $v_L \sim L^{3/5}$ and $\rho_L \sim L^{-4/5}$. This produces the fractal dimension $D = 2.2$. It should be emphasized again that all these scenarios assume a quasi-stationary regime.

However, numerical simulations of molecular cloud fragmentation have been, so far, carried out in dissipative schemes which allow for efficient clumping (e.g Klessen et al 1998, Monaghan & Lattanzio 1991). As such, they do not reach stationary states. Our approach is to add an energy input making up for the dissipative loss. After relaxation from initial conditions we attempt to reach a fragmented but non-collapsing state of the medium that does not decay into homogeneous or centrally condensed states. It is then meaningful to compute the velocity and density fields power spectra and test the standard theoretical assumptions. It is also an opportunity to investigate the possible fractal structure of the gas. Indeed, starting from a weakly perturbed homogeneous density field, the formation time of a fractal density field independent of the initial conditions is at the very least of the order of the free-fall time, and more likely many times longer. A long

integration time should permit full apparition of a fractal mass distribution, independent of the initial conditions.

This program encounters both standard and specific difficulties. Galaxies clustering as well as ISM clumping require large density contrasts, that is to say high spatial resolution in numerical simulations. This point is tackled, be it uneasily, by adaptative-mesh algorithms or tree algorithms, or multi-scale schemes (P^3M). Another problem is the need for higher time resolution in collapsed region. This is CPU-time consuming or is dealt with by multiple time steps. This point is of primary sensitivity in our simulation since we need to follow accurately the internal dynamics of the clumps and filaments to avoid total energy divergence. Finally we need a long integration time to reach the stationary state. This is directly in competition for CPU-time with spatial resolution for given computing resources.

2. Numerical methods

2.1. Self-gravity

In our simulation we use N-body dynamics with a hierarchical tree algorithm and multipole expansion to compute the forces, as designed by Barnes & Hut (1986, 1989). The number of particles is between 10 000 and 120 000 particles. We are limited by the fact that we need long integration time in our study.

Within the N-body framework the tree algorithm is a $N \ln(N)$ search algorithm picking the closest neighbours for exact force computation and sorting farther out particles in hierarchical boxes for multipole expansion. The size of the boxes used in the expansion is set, for the contribution of a given region to the force, by a control parameter θ defining the maximal angular size of the boxes seen from the point where the force is computed. Typical values used for θ are 0.5 to 1.0. Multipole expansion is carried out to quadrupole terms. As usual a short distance softening is used in the contribution of the closest particle to the interaction. The softening length is taken as $\sim 1/10$ of the inter-particle distance of the homogeneous state.

2.2. Boundary conditions

There are two ways to erase the finite size effect and avoid spherical collapse in a N-body simulation. We can choose either quasi-periodic boundary conditions or fully periodic boundary conditions following Ewald method (Hernquist et al 1991). In quasi-periodic conditions the interaction of two particles is computed between the first particle and the closest of all the replicas of the other particle. The replicas are generated in the periodization of the simulation box to the whole space. In the fully periodic conditions, the first particle interacts with all the replicas of the other one. The relevance of each method will be discussed in section 3.1. We will compare them for simple free-falls using the fractal dimension as diagnosis.

2.3. Time integration and initial conditions

The integration is carried out through a multiple time steps leap-frog scheme. Making a Keplerian assumption about the orbits of the particles, we have the following relation between time step and the local interparticle distance: $\delta\tau \sim (\delta l)^{\frac{3}{2}}$. In a fractal medium, the exponent could be different. We do not take this into account since it would lead us to modify the integration scheme dynamically according to the fractal properties of the system. As the tree sorts particles in cells of size $2^n d_0$ according to the local density, we should use $(2\sqrt{2})^n \delta t_0$ time steps. For simplicity we are using $3^n \delta t_0$. Then, n different time steps allow us to follow the dynamics with the same accuracy over regions with density contrasts as high as $2^{3(n-1)}$.

We will use several types of initial conditions. The usual power law for the density power spectrum will be used for the free falls. It is usually implemented by using Zel'dovitch approximation which is valid before first shell crossing for a pressureless perfect fluid. The validity range of this approximation is difficult to assess in an N-body simulation. We use a similar implementation that does not however extend to non-linear regimes but also gives density power spectra with the desired shapes. A gaussian velocity field is chosen with a specified power spectrum $P_v(k) \sim k^{\alpha-2}$, then the particles are positioned at the nodes of a grid and displaced according to the velocity field with one time step. The resulting density fluctuations spectrum is $P_\rho(k) \sim k^\alpha$ according to the matter conservation.

2.4. Gas physics

There can be several modelizations for the ISM: either it is considered as a continuous and fluid medium and simulated through gas hydrodynamics (with pressure, shocks, etc..) or, given the highly clumped nature of the interstellar medium, and its highly inhomogeneous structure (density variations over 6 orders of magnitude), it can be considered as a collection of dense fragments, that dissipate their relative energy through collisions. Our choice of particle dynamics assumes that each particle stands for a clump and neglects the interclump medium. Another reason is that we expect a fractal distribution of the masses. This means a non-analytical density field which is not to be easily handled by hydrodynamical codes.

The dissipation enters the dynamics through a grid-less sticky particles collision scheme. The collision round is periodically computed every 1 to 10 time steps. The frequency of this collision round is one way to adjust the strength of the dissipation. Since, as the precise collision schemes will reveal, we adopt a statistical treatment of the dissipation, it is not necessary to compute the collision round at each time step. Two schemes are investigated. The first uses the tree search to find a candidate to collision with a given particle, in a sphere whose radius r_c is

a fixed parameter. Inelastic collisions are then computed, dissipating energy but conserving linear momentum. In the second scheme, each particle has a probability to collide proportional to the inverse of the local mean collision time. If it passes the probability test, the collision is computed with the most suitable neighbour. In this second scheme, dissipation may occur even in low density regions; in the first it occurs only above a given density threshold. In practice this implies that, in the first scheme, dissipation happens only at small scales, while in the second, it happens on all scales but is still stronger at small scales.

Special attention must be paid to the existence of a small scale cutoff in the physics of the system. Indeed, at very small scale (~ 20 AU), the gas is quasi-adiabatic. Its cooling time is then much longer than the isothermal free fall time at the same scale. Moreover, the mean collision time between clumps at this scale, in a fractal medium, is much shorter than the cooling time. As a result, collisions completely prevent the already slowed down processes of collapse and fragmentation in the quasi-adiabatic gas: the fractal structure is broken at the corresponding scale. To take these phenomena into account in our simulation, we need to introduce a large-density cutoff. This is achieved by computing elastic or super-elastic collisions at scale $< 0.5r_c$, instead of inelastic collisions. The practical implementation follows the same procedure as for the first inelastic collision scheme. In the case of super-elastic collisions, the overall energy balance is still negative at small scales (due to a volume effect), however we do introduce a mechanism of energy injection at small scale. This choice can be furthermore justified by physical considerations.

When there is no energy provided by star formation (for example in the outer parts of galaxies, where gas extends radially much beyond the stellar disk), the gas is only interacting with the intergalactic radiation field, and the cosmic background radiation. The latter provides a minimum temperature for the gas, and plays the role of a thermostat (at the temperature of 2.76K at zero redshift). The interaction between the background and the gas can only occur at the smallest scale of the fragmentation of the medium, corresponding to our small scale cutoff; the radiative processes involve hydrogen and other more heavy elements (Combes & Pfenniger 1997). To maintain the gas isothermal therefore requires some energy input at the smallest scale.

Several schemes for the energy input have been tried. Reinjection at small scale through added thermal motion has proved unable to sustain the system in any other state than an homogeneous one. Then, turning to the turbulent point of view, we have tried reinjection at large scale. Two main methods have been tested; reinjection through a large scale random force field, and reinjection through the action of the galactic shear. Their effect will be discussed in section 5.

Finally, the statistical properties of the system can be described in many different way. We will use the correla-

tion fractal dimension as diagnosis. Definition and example of application of this tool are given in the appendix.

3. Simple 3-D free falls

3.1. The choice of the boundary conditions

A fractal structure such as observed in the ISM or in the galaxies distribution obeys a statistical translational invariance. If we run simulations with vacuum boundary condition, this invariance is grossly broken. On the other hand the quasi-periodic or fully-periodic conditions restore this invariance to some extent. They have been used in cosmological simulations. Hernquist et al (1991) have compared the two models to analytical results and found that the fully-periodic model simulates more accurately the self-gravitating gas in an expanding universe. This is in agreement with expectations, since uniform expansion is automatically included in a fully-periodic model, while it is not in a quasi-periodic one. Klessen (1996,1998) applied Ewald method to simulations of the interstellar medium. This is not natural since expansion is necessary to validate Ewald method. Nevertheless one can argue that the dynamics is not altered by the use of Ewald method in regions with high density contrasts.

Hernquist's study was on the dynamics of the modes. We are more interested in the fractal properties. As far as we are concerned the question is whether the same initial conditions produce the same fractal properties in a cosmological framework (fully-periodic conditions) and in a ISM framework (quasi-periodic conditions). We will try to answer this question in section 3.3.

3.2. The choice of the initial conditions

The power spectrum of the density fluctuations is most commonly described as a power law in cosmological simulations. Then, different exponents in the power law produce different fractal dimensions. The cosmologist can hope to find the fractal dimension from observations and go back to the initial power spectrum. In the case of the interstellar medium however, it is unlikely that the fractal dimension is the result of initial conditions since the lifetime of the medium is much longer than the dynamical time of the structures. In this regard, all initial conditions should be erased and produce the same fractal dimension. We will check whether this is the case for power law density spectra with different exponents. Simple free falls with such initial conditions will allow the comparison between the two types of periodic boundary conditions and will allow us to compare between 3D and 2D models and different dissipation schemes.

3.3. Simulations and results

The four first simulations are free falls from power law initial conditions in either fully or quasi-periodic boundary

conditions for two different power law exponents: $\alpha = -1$ and $\alpha = -2$. About 120 000 particles were used in the simulations. The time evolution of the particle distribution for $\alpha = -2$ and fully periodic condition is plotted in Fig. 1. If we compare the qualitative aspect of the matter distribution with those found in SPH simulations (Klessen 1998), a difference appears. Filaments are less present in this N-body simulation than in SPH simulations. We believe that this is due to the strongly dissipative nature of SPH simulations. Indeed filaments form automatically, even *without gravity*, with $P(k) \sim k^{-2}$ initial conditions for the density field. Then, the strong dissipation of SPH codes is necessary to retain them; N-body codes seem to show that gravity by itself is not enough.

3.3.1. Fractal dimension

For each of the four simulations, the fractal dimension as a function of scale has been computed at different times of the free fall. Results are summarized in Fig. 2.

The fractal dimension of a mathematical fractal would appear either as an horizontal straight line or as a curve oscillating around the fractal dimension if the fractal has no randomization (like a Cantor set). For our system, it appears that at sufficiently early stages of the free fall, and for scales above the dissipative cutoff, the matter distribution is indeed fractal. However the dimension goes down with time to reach values of 2 for $\alpha = -2$, and between 2 and 2.5 for $\alpha = -1$. This is the fractal dimension for the total density, not for the fluctuations only. Stabilization of the fractal dimension marginally happens before the dissipation breaks the fractal.

One conclusion is however reasonable: as far as the fractal dimension is concerned, the difference between fully-periodic boundary conditions and quasi-periodic boundary conditions is not important. The deviation is a bit stronger in the $\alpha = -1$ case, which is understandable since $\alpha = -1$ produces weaker density contrasts in the initial conditions than $\alpha = -2$ and so the dynamics is less decoupled from the expansion. The effect of this conclusion is that we will not use the fully-periodic boundary conditions in further simulations since they require more CPU time and have no physical ground in the ISM framework. Clump mass spectra are given in appendix B.

4. Simple 2-D free falls

We consider a 2-D system where particles have only two cartesian space coordinates but still obey a $\frac{1}{r^2}$ interaction force.

4.1. Motivations for the two dimensional study

Turning to 2-D simulations allows access, for given computing resources, to a wider scale-range of the dynamics. Or, for given computing resources and a given scale-range,

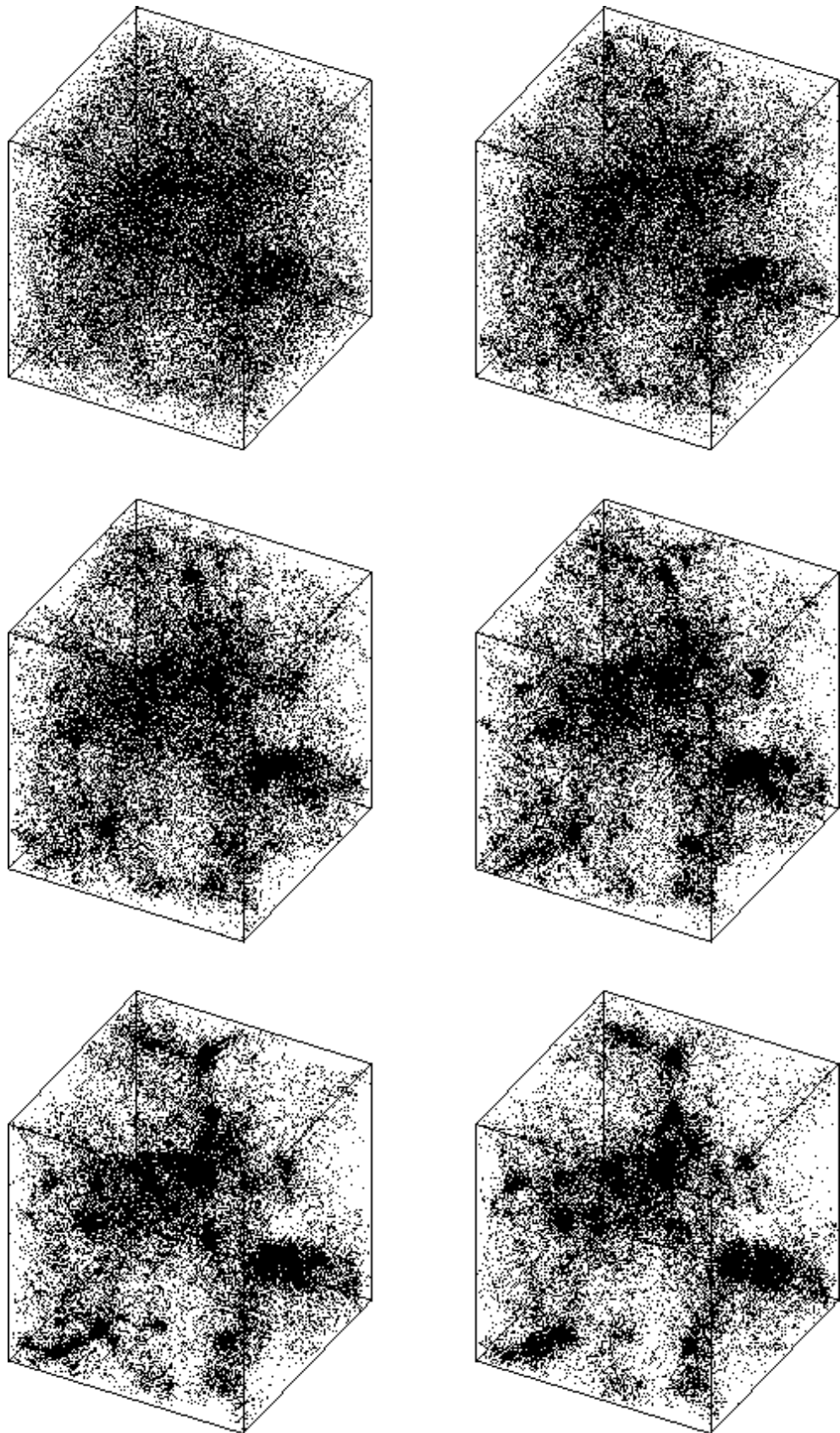


Fig. 1. Time evolution over about 0.5 free fall time. The initial conditions are density fluctuations with power spectrum $P(k) \sim k^{-2}$. The simulation contains 117649 (49^3) particles.

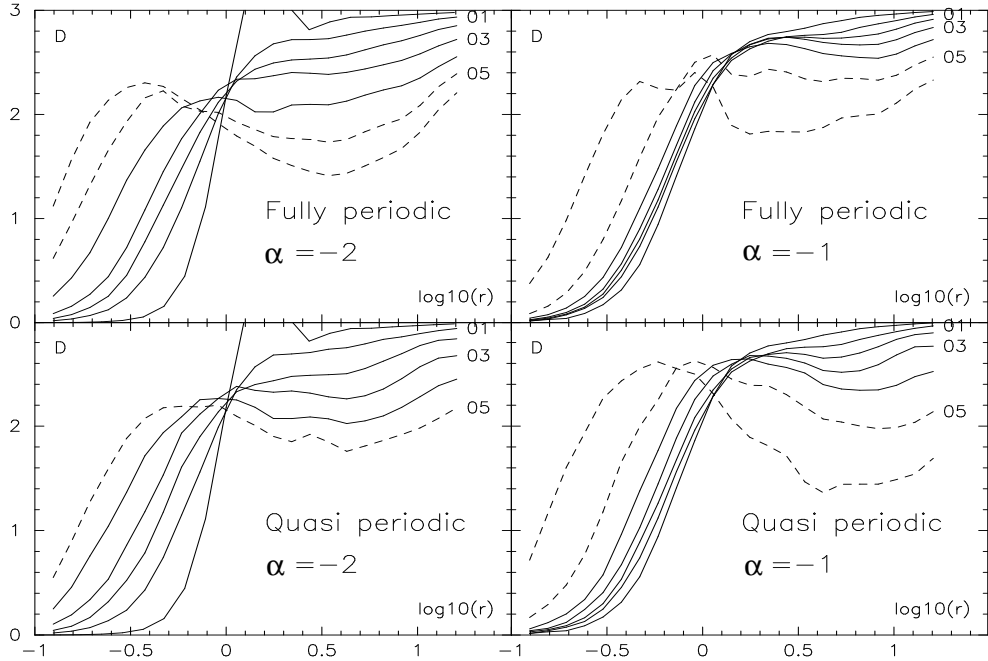


Fig. 2. The fractal dimension of the matter distribution is plotted as a function of the log of the scale at different times of the free fall in four different conditions described under the curves. α designates the exponent of the power law of the density power spectrum. Curves are labeled from early to late states.

to larger integration times. The later is what we will need in the simulation with energy injection. In practice we will choose to use 10^4 particles in 2-D simulations to access both a larger integration time and a wider scale range. Indeed, between a 3-D simulation with $N = 10^5$ particles and a 2-D simulation with 10^4 particles one improves the scale range from $[1, N^{\frac{1}{3}} = 46]$ to $[1, N^{\frac{1}{2}} = 100]$. At the same time one can increase the integration-time by a factor of ~ 10 at equal CPU cost.

We can also add a physical reason to these computational justifications. The simulations with an energy injection aim to describe the behaviour of molecular clouds in the thin galactic disk. This medium has a strong anisotropy between the two dimensions in the galactic plane and the third one. As such it is a suitable candidate for a bidimensional modeling.

Moreover, studying a bidimensional system will allow us to check how the fractal dimension, dependent or not of the initial conditions, is affected by dimension of the space.

4.2. Simulations with 2 different dissipative schemes

Here again initial conditions with a power law density power spectrum are used. Exponent $\alpha = -2$ is chosen to allow a comparison with the 3-D simulations. Boundary conditions are quasi-periodic. We have carried out two simulations with the two different dissipative schemes de-

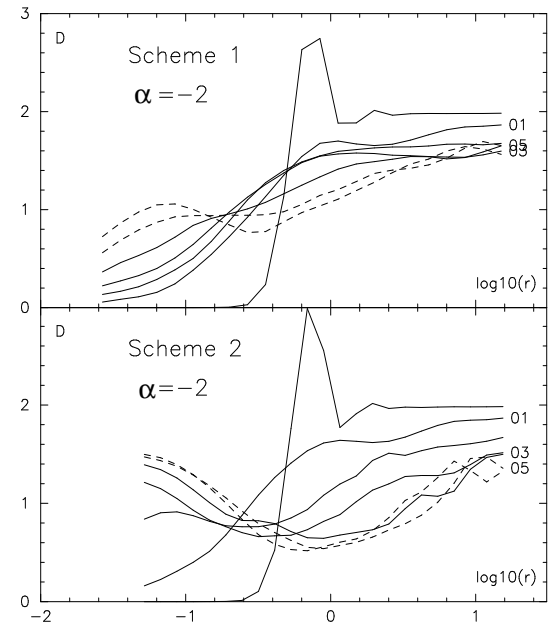


Fig. 3. Fractal dimension as function of scale at different stages of the time evolution. The simulations are two-dimensional with 10609 particles. The dissipative scheme is modified between the two simulations according to the description in sec 2.4 .

scribed in section 2.4 . The fractal dimensions at different stages of each of these two simulations are shown in Fig. 3.

In both simulations the fractal dimension of the homogeneous initial density field is 2 at scales above mean inter-particle distance and 0 below. Then the density fluctuations develop and the fractal dimension goes down to about 1.5 – 1.6 in both simulations. This value was not reached in 3-D simulations. This shows that the dimension of the space has an influence on the fractal dimension of a self-gravitating system evolved from initial density fields with a power law power spectrum. Indeed spherical configurations are favoured in 3 dimensions and may produce a different type of fractal than cylindrical configurations which are favored in two dimensions.

Another point is that the fractal dimension of the system at small scales is indeed sensitive to the dissipative scheme. The second scheme even alters the fractality of large scales. So even if we believe that the fractality of a self-gravitating system is controlled by gravity, we must keep in mind the fact that the dissipation has an influence on the result. In this regard, discrepancies should appear between N -body simulations including SPH or other codes.

The clump mass spectra are not conclusive due to insufficient number of clumps formed with 10609 particles.

5. 2-D simulations with an energy source

As already stated, the ISM is a dissipative medium. Structures radiate their energy in a time-scale much shorter than the GMCs typical life time inferred from observations. Therefore we are led to provide an energy source in the system to obtain a life time longer than the free fall time.

5.1. The choice of the energy source

Different types of sources are invoked to provide the necessary energy input: stellar winds, shock waves, heating from a thermostat, galactic shear... We have tested several possibilities.

Our first idea was to model an interaction with a thermostat by adding periodically a small random component to the velocity field. We have tried to add it either to all the particles or only to the particle in the cool regions. If enough energy is put into this random injection, the mono-clump collapse is avoided. However the resulting final state is not fractal, nor does it show density structures on several different scales. It consists in a few condensed points, like "blackholes", in a hot homogeneous phase.

The second idea is to model a generic large scale injection by introducing a large scale random force field. We have tried stationary and fluctuating fields. It is possible in this scheme, by tuning the input and the dissipation, to lengthen the medium life time in an "interesting" inhomogenous state by a factor 2 or 3. However the final state, after a few dynamical times, is the same as for thermal input.

We would like to emphasize that, in all the cases just mentioned, the existence of super-elastic collisions at very short distances, are *not at all* able to avoid the collapse of "blackholes". They are indeed beaten by inelastic collisions which happen more frequently. Thus the density cutoff introduced by superelastic collision, is not able all by itself to sustain or destroy clumps.

Only one of the schemes we have tested avoids the blackhole/homogeneity duality. In this scheme, energy is provided by the galactic shear. It produces an inhomogeneous state whose life time does not appear to be limited by a final collapse in the simulations. We now describe this scheme in detail.

5.2. Modelisation of the galactic shear

The idea is to consider the simulation box as a small part of a bigger system in differential rotation. The dynamics of such a sub-system has been studied in the field of planetary systems formation (Wisdom and Tremaine 1988). Toomre (1981) and recently Hubert and Pfenniger (1999) have applied it to galactic dynamics.

The simulation box is a rotating frame with angular speed Ω_0 which is the galactic angular speed at the center of the box. Coriolis force acts on the particles moving in the box. An additional external force arises from the discrepancy between the inertial force and the local mean gravitational attraction of the galaxy. The balance between these two forces is achieved only at points that are equally distant from the galactic center as the center of the box. Let us consider a 2-dimensional case. If y is the orthoradial direction, and x the radial direction the equations of motion are written:

$$\begin{aligned}\ddot{y} &= -2\Omega_0\dot{x} + F_y \\ \ddot{x} &= 2\Omega_0\dot{y} - 2\Omega_0r_0 \left. \frac{d\Omega}{dr} \right|_{r_0} x + F_x\end{aligned}$$

The $F_{x,y}$ are the projections of the internal gravitational forces. The shear force acting in the radial direction is able to inject into the system energy taken from the rotation of the galaxy as a whole.

Some modifications must also be brought to the boundary condition. It is not consistent with the differential rotation to keep a strict spatial periodicity. To take differential rotation into account, layers of cells at different radii must slide according to the variation of the galactic angular speed between them. One particle still interacts with the closest of the replicas of another particle (including the particle itself). This is sketched on Fig. 4.

5.3. Results

We have computed simulations in two dimensions with 10609 particles. The direction orthogonal to the galactic

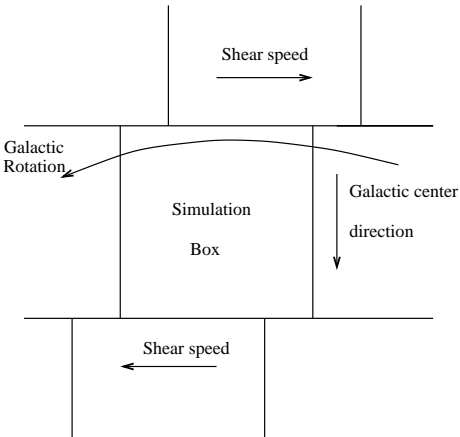


Fig. 4. Effect of the galactic shear on the periodic conditions. The layers of cells have a relative drifting speed.

disk is not taken into account. A tuning between dissipation rate and shear strength is necessary to obtain a structured but non collapsing configuration. However it is not a fine tuning at all. We found out that, in a range of values of the shear, the dissipation adapts itself to compensate the energy input so that we didn't encounter any limitation in the life time of the medium. The simulations have been carried out over more than 20 free-fall times. Snapshots from a simulation are plotted in Fig. 5.

5.3.1. Formation of persistent structures

We can see that tilted stripes appear in the density field. This structure appears also in simulations by Toomre (1981) and Hubert and Pfenniger (1999). The new feature is the intermittent appearance of dense clumps within the stripes. These clumps remain for a few free fall times of the total system, then disappear, torn apart by the shear. This phenomenon is unknown in the simple free fall simulations where a clump, once formed, gets denser and more massive with time. It also appeared that the tearing of the clumps by the shear happens only if super-elastic collisions enact an efficient density cut-off. If we use elastic collisions only, below the dissipation scale, thus enacting a less efficient density cut-off, the clumps persist. However they do not collapse to the dense blackhole states encountered with different large scale energy input schemes. So the combination of the galactic shear and super-elastic collisions below the dissipation scale is necessary to obtain destroyable clumps, while the shear alone produces rather stable clumps, and the super-elastic collisions alone cannot avoid complete collapse.

While we cannot consider the density field as a fractal structure, it is indeed the beginning of a hierarchical fragmentation since we have two levels of structures. However the stripes are mainly the result of the shear. On the other hand the clumps are the simple gravitational fragmenta-

tion of the stripes. These two structures are not created by the exact same dynamical processes.

It must also be noted that the shear plays a direct role at large scale (of the order of 10 pc), where the galactic tidal forces are comparable to the self-gravity forces of the corresponding structures. But since the structures are fragmenting hierarchically, it is expected that its effect propagates and cascades down to the smallest scales.

5.3.2. Fractal analysis

The fractal dimension of the medium is plotted at different times in Fig. 6. Two characteristic scales are clearly visible. At large scale, the scale of the stripes, the dimension is about 1.9 with some fluctuations in time. At small scale, the dimension fluctuates strongly due to the appearance and disappearance of clumps. This shows through the appearance of a bump at the clump size. This size is about the dissipation scale. It is important to mention that the small scale range, while under the cutoff of the initial homogeneous condition, is not under our dynamical resolution. The mean inter-particle distance decreases from its initial value and is consistently followed by the N -body dynamics.

5.3.3. Effect of the initial conditions

We have already emphasized that in GMC simulations, the resulting structure should be independent of the initial conditions. We have performed the simulation for various values of the exponent of the power spectrum. In the range $[-0.5, 0.5]$ the long time behaviour is the one described above, thus satisfying the required independence. However, for more steep spectrum value like -2, the medium tend to collapse early into large clumps, thereby preventing the shear to act efficiently.

We see that the behaviour is independent of the initial conditions as long as the continuity of the medium at scale larger than the GMC size (the clump size in the simulation) is not broken so that the shear can act to sustain the GMC against collapse.

6. Discussion and Conclusion

We have shown that, in simulations without energy input, the evolution of the fractal dimension depends on the initial conditions and also, to some extent, on the dissipation schemes. Then we have investigated the effects of an energy input on the dynamics of the system. This input is necessary to prevent the total collapse of the system. Moreover, we do not want the input to destroy the inhomogeneous fractal structure of the medium, as done by random reinjections (thermal bath, random force field). Among the solutions we have tested, only the highly regular force field provided by the galactic shear preserves an inhomogeneous state. However this state is

quite strongly constrained by the geometry of the shear. Stripes appear as a result. Interestingly, clumps are formed in these stripes and can be destroyed if we have an efficient enough density cutoff.

This state does not have a well-defined fractal dimension. Stripes are the effect of a large scale action on the system and within our dynamic range in scale, we cannot get rid of this boundary effect. If we had more resolution, the clumps could fragment, and we might reach a scale domain free of boundary effects. One of our prospects is to follow the inner dynamic of a clump with simulations in recursive sub-boxes going down in scale. This can produce a great dynamic scale range but only in a small region of space.

Appendix A: Computing the fractal dimension

By fractal dimension we mean more accurately the correlation fractal dimension. We will use the notation D_f , defined as follows : if we consider a fractal set of points of equal weight located at \mathbf{x}_j , the fractal dimension of the ensemble obeys the relation :

$$\lim_{r \rightarrow 0} r^{D_f} = \lim_{r \rightarrow 0} \left\langle \sum_j \int_{|\mathbf{x} - \mathbf{x}_i| < r} \delta(\mathbf{x} - \mathbf{x}_j) d\mathbf{x} \right\rangle_i.$$

The brackets stand for an ensemble average. In computational applications and in physical systems, the $r \rightarrow 0$ limit is not reached. However the relation should hold at scales where the boundary effects created by the finite size of the system are negligible.

In practice, for a non-fractal ensemble of points, D_f usually depends on r (but not always). For a fractal it is independent of r , or at least it oscillates around a mean value. The latter case can happen for a set with a strong scale periodicity like the Cantor set. Examples are given in Fig. A.1. As the above remarks show, D_f is not a definitive criterion of fractality.

According to the definition, the computation of the fractal dimension is based on the following method. r^{D_f} is the mean mass in a sphere of radius r centered on a particle. This mass is actually computed for each particle using the tree search, then it is averaged and the value $D_f(r)$ is derived. The average can be made on a subset of points to lower the computation cost, the result is then noisier.

Appendix B: Clump mass spectrum

Although the results are not very conclusive, we give the mass distribution of the clumps in the 3-D simple freefall, to allow comparison with observational data and other numerical simulations. Plotting $\log_{10}(N)$ against $\log_{10}(m)$, the slope inferred from observation data is -0.5 . Thus the clump mass spectrum behaves as a power law : $\frac{dN}{dm} \sim m^{-1.5}$.

Fig. B.1. Clump mass spectra for two values of α at different evolution times. The given time-unit is about $1/10$ of the free fall time. At $t = 5$, the spectra show a -0.38 ± 0.03 slope for $\alpha = -1$ and a -0.18 ± 0.03 for $\alpha = -2$.

To produce the mass spectrum, the first step is to define individual clumps. We have used an algorithm very similar to the one proposed by Williams et al (1994). We compute the density field from an interpolation of the distribution of the particles with a cloud-in-cell scheme. It should be mentioned that this procedure tends to produce an artificially high number of very small clumps associated to isolated particles or pair of particles which should not be considered as clumps at all.

On Fig. B.1 the clump mass spectrum is given at different times of the evolution and for the two types of initial conditions ($\alpha = -1, -2$). Quasi-periodic boundary conditions are used. As time increases, as we can see, the clump mass spectrum slope decreases to reach -0.38 ± 0.03 for $\alpha = -1$ and -0.18 ± 0.03 for $\alpha = -2$. At later times, the power law is broken by the final dissipative collapse. According to this diagnosis, the case $\alpha = -1$ is closer to the observed values. However, once again, this simulation provides only a transient state which is unlikely to be a good model of a GMC.

References

Barnes J., Hut P.: 1986, Nature 324, 446
 Barnes J., Hut P.: 1989, ApJS 70, 389
 Boss A.: 1997, ApJ 483, 309
 Burkert A., Bate M.R., Bodenheimer P.: 1997, MNRAS 289, 497
 Combes F., Pfenniger D.: 1997, A&A 327, 453
 de Vega H., Sanchez N., Combes F.: 1996, Nature 383, 53
 Diamond P.J., Goss W.M., Romney J.D. et al: 1989, ApJ 347, 302
 Faison M.D., Goss W.M., Diamond P.J., Taylor G.B.: 1998, AJ 116, 2916
 Falgarone E., Puget J-L., Perault M.: 1992, A&A 257, 715
 Fiedler R.L., Dennison B., Johnston K., Hewish A.: 1987, Nature 326, 6765
 Fiedler R.L., Pauls T., Johnston K., Dennison B.: 1994, ApJ 430, 595
 Fleck R.C.: 1981, ApJ 246, L151
 Heithausen A., Bensch F., Stutzki J., Falgarone E., Panis J.F.: 1998, A&A 331, L65
 Hernquist L., Bouchet F., Suto Y.: 1991, ApJS 75, 231
 Hoyle F.: 1953, ApJ 118, 513
 Huber D., Pfenniger D.: 1999, astro-ph/9904209, to be published in the proceedings of The Evolution of Galaxies on Cosmological Timescale, eds. J.E. Beckman & T.J. Mahoney, Astrophysics and Space Science.
 Klessen R. S.: 1997, MNRAS , 11
 Klessen R. S., Burkert A., Bate M.R.: 1998, ApJ 501, L205
 Klessen R. S., Burkert A.: 1999, astro-ph/9904090 submitted to ApJ.

Larson R.B.: 1981, MNRAS 194, 809
Monaghan J.J., Lattanzio J.C.: 1991, ApJ 375, 177
Norman C.A., Silk J.: 1980, ApJ 238, 158
Pfenniger D., Combes F.: 1994, A&A 285, 94
Rees M.J., 1976, MNRAS 176, 483
Scalo J.M.: 1985, in "Protostars and Planets II", ed. D.C. Black
and M.S. Matthews, Univ. of Arizona Press, Tucson, p. 201
Toomre A.: 1981, in "The Structure and Evolution of Normal
Galaxies", eds. Fall S.M. and Lynden-Bell D., Cambridge
Univ. Press, p. 111
Wisdom J., Tremaine S., 1988, Astron. J., 95, 925
Williams J. P., De Geus E. J., Blitz L.: 1994, ApJ 428, 693

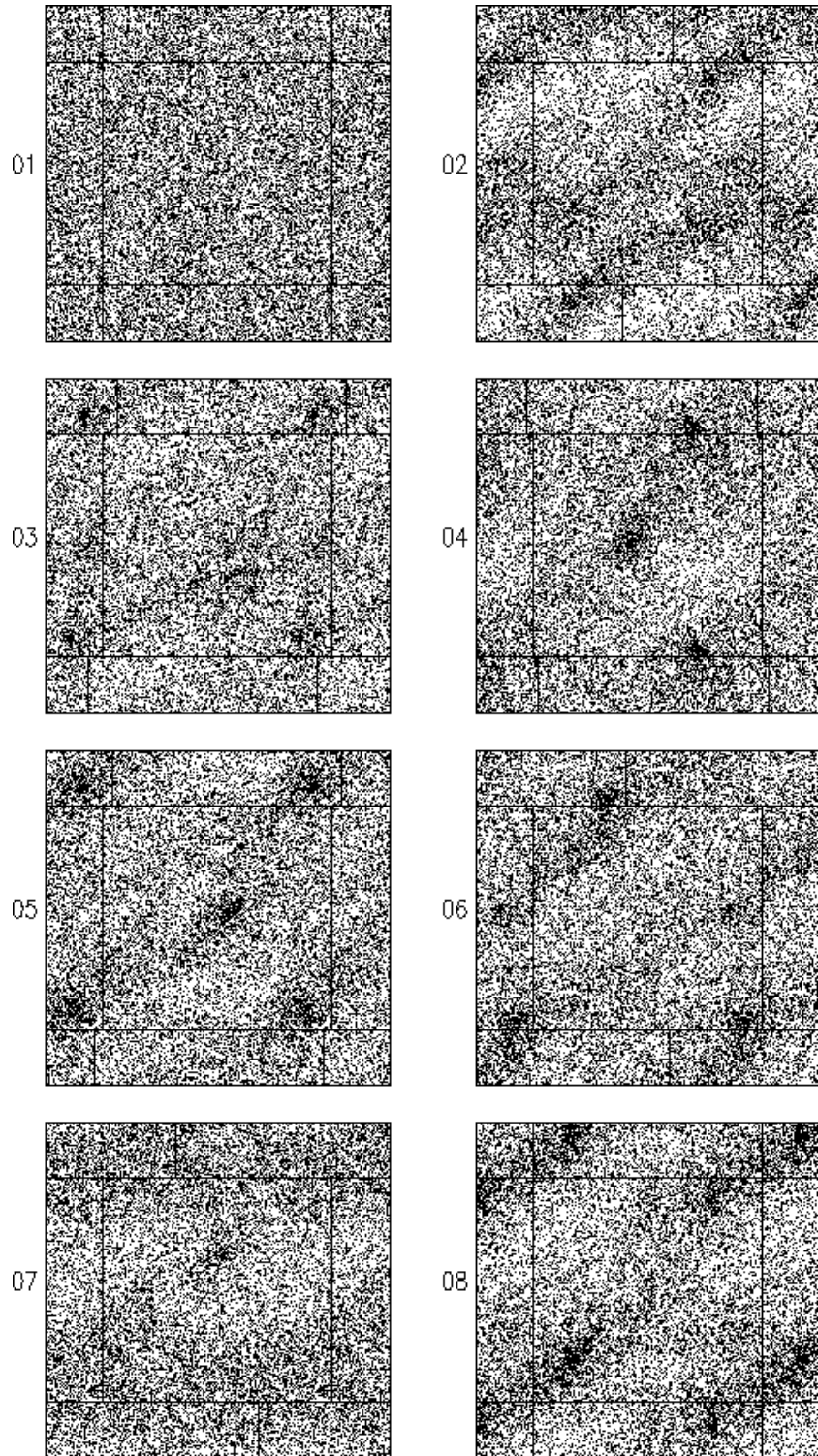


Fig. 5. 2-D simulation with 10609 particles over 20 free fall times of the total system. The different snapshots are taken at periodic time interval. The galactic center is toward the bottom of the boxes. Sliding replicas of the central box are shown for continuation

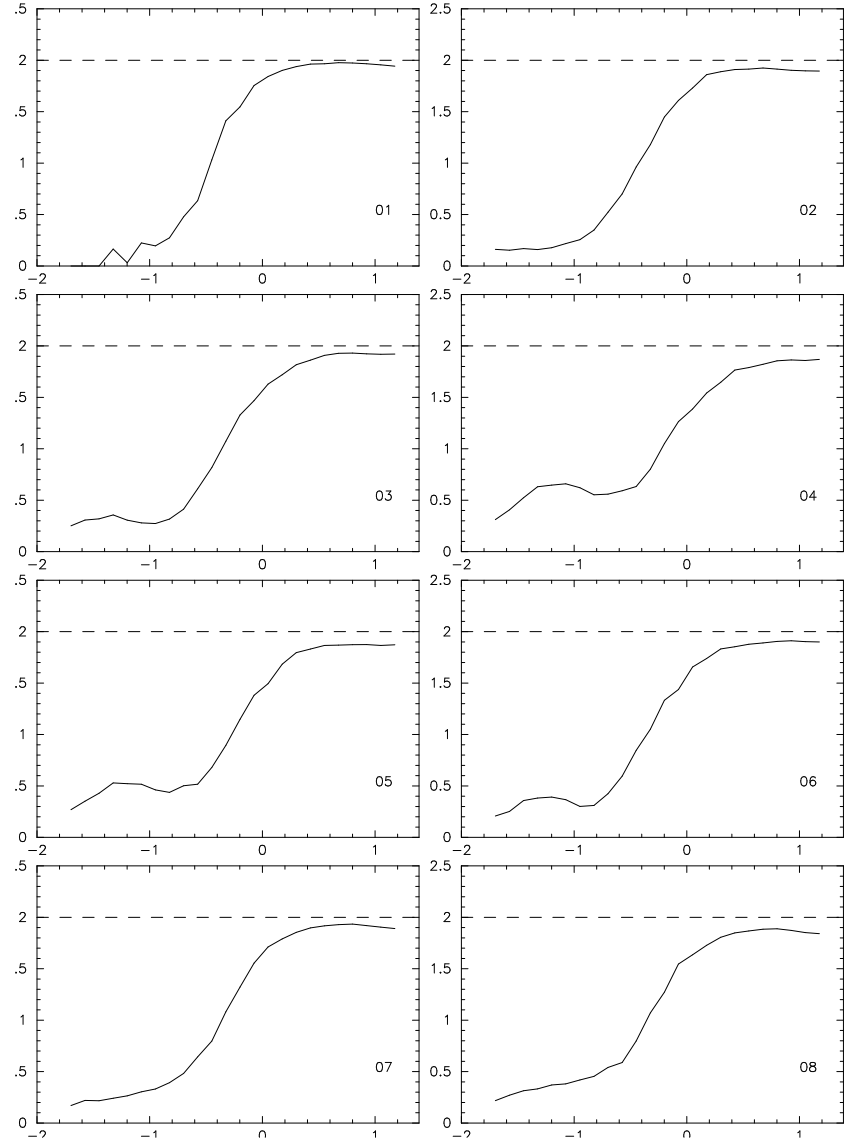


Fig. 6. Fractal dimension computed at different epochs matching those of fig 5.

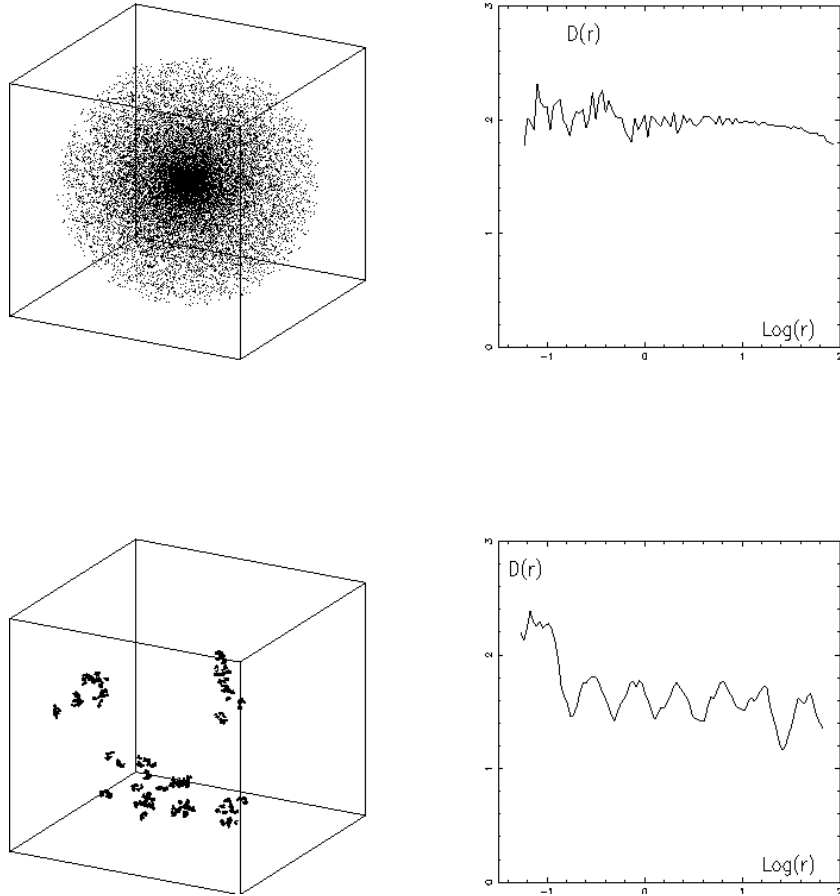


Fig. A.1. The fractal correlation dimension is plotted as a function of the scale for two different sets of points : the first (not fractal) set is an isothermal sphere and a second is a fractal cantor-like set build recursively on 8 levels with a small part of randomization. This shows that D_f independent of r is neither a sufficient nor a necessary condition of fractality